◆ Human Brain Mapping 5:280–286(1997) ◆

Retinotopic Organization of Early Visual Spatial Attention Effects as Revealed by PET and ERPs

M.G. Woldorff,* P.T. Fox, M. Matzke, J.L. Lancaster, S. Veeraswamy, F. Zamarripa, M. Seabolt, T. Glass, J.H. Gao, C.C. Martin, and P. Jerabek

Research Imaging Center, UTHSCSA, San Antonio, Texas 78284-6240

Abstract: Cerebral blood flow PET scans and high-density event-related potentials (ERPs) were recorded (separate sessions) while subjects viewed rapidly-presented, lower-visual-field, bilateral stimuli. Active attention to a designated side of the stimuli (relative to passive-viewing conditions) resulted in an enhanced ERP positivity (P1 effect) from 80–150 msec over occipital scalp areas contralateral to the direction of attention. In PET scans, active attention vs. passive showed strong activation in the contralateral dorsal occipital cortex, thus following the retinotopic organization of the early extrastriate visual sensory areas, with some weaker activation in the contralateral fusiform. Dipole modeling seeded by the dorsal occipital PET foci yielded an excellent fit for the P1 attention effect. In contrast, dipoles constrained to the fusiform foci fit the P1 effect poorly, and, when the location constraints were released, moved upward to the dorsal occipital locations during iterative dipole fitting. These results argue that the early ERP P1 attention effects for lower-visual-field stimuli arise mainly from these dorsal occipital areas and thus also follow the retinotopic organization of the visual sensory input pathways. These combined PET/ERP data therefore provide strong evidence that sustained visual spatial attention results in a preset, top-down biasing of the early sensory input channels in a retinotopically organized way. *Hum. Brain Mapping 5:280–286, 1997.*

Key words: positron emission tomography; event-related potentials; visual cortex; neuroimaging; visual attention; dipole modeling; extrastriate cortex; cerebral blood flow; retinotopy; selective attention

INTRODUCTION

Functional brain imaging studies using positron emission tomography (PET) and, more recently, functional magnetic resonance imaging (fMRI) have indicated specific areas of the brain as being involved in visual attention [reviewed in Posner and Raichle, 1994]. Such hemodynamically-based imaging studies, however, require integrating tracer activity over a period of many seconds and thus provide no characterization of the *timing* of information processing in the brain. Event-related potentials (ERPs), on the other hand, reflect the rapidly changing electrical activity in the brain evoked by a stimulus or cognitive event and thus provide high temporal resolution images of neuronal populations engaged in information processing [reviewed in Hillyard and Picton, 1987; Hillyard et al., 1995]. Specifying the neural sources of the various ERP effects, however, has been difficult.

One recent study combined ERP and PET to study lateralized visual spatial attention to bilateral stimuli presented to the upper visual field [Heinze et al., 1994]. Attending to either the left or right side of these stimuli

*Correspondence to: Marty G. Woldorff, Ph.D., Research Imaging Center, University of Texas Health Science Center, 7703 Floyd Curl Drive, San Antonio, TX 78240-6240. E-mail: mwoldorff@uthscsa.edu

Received for publication 12 May 1997; accepted 12 May 1997

resulted in enhanced PET activity in the contralateral fusiform gyrus, which was experimentally associated with an early (90–140 msec) attention-enhanced ERP positivity over the contralateral occipital cortex (the P1 effect). By use of dipole modeling, including ''seeding'' the source analysis of the ERP effect with the PET locations, the authors found that these ventral occipital locations appeared to be a likely source for the P1 effect.

In the present study, PET and high-density (64-channel) ERPs were combined to study lateralized attention to bilateral stimuli in the *lower visual field* to examine further the organization of spatial attention effects. Various sources of evidence, e.g., neuropsychological lesion research and nonhuman primate work [reviewed in Zeki, 1993] and functional brain imaging studies [e.g., Sereno et al., 1995], indicate a clear retinotopic organization to the processing in the early visual sensory areas. More specifically, there is contralaterality to the representation in these areas (left visual field is processed in the right occipital cortex and right field on the left); in addition, the upper visual field is processed in the ventral occipital cortex (below the calcarine fissure), and the lower field in the dorsal occipital cortex (above the calcarine). After these earliest visual occipital areas that have a dorsal/ventral split retinotopic representation, visual processing (for higher-level visual object analysis) appears to proceed into the ventral occipital and temporal brain regions for both the upper and lower fields (the ''ventral processing stream,'' reviewed in Ungerleider and Haxby [1994]). Thus, the key question here, especially vis-à-vis the study of Heinze et al. [1994], is whether the effects of attention would follow the retinotopic organization of the early occipital visual processing areas. That is, would the occipital PET attentional enhancement effects in the present study now be mainly in the contralateral *dorsal* occipital cortex due to the use of lower-visual-field stimuli? Moreover, would the estimated source for the P1 effect follow this pattern as well (i.e., be localized to the dorsal occipital cortex), thereby covarying with the PET effects?

METHODS

Stimuli and task

In separate sessions, subjects (n = 10, age 18–41 years, all right-handed, 4 male) performed identical visual attention tasks while either ERPs or PET scans of their brain activity were recorded. In all conditions, subjects fixated on a small cross in the center of the screen (50 cm away) while bilateral stimuli of 150-msec duration were rapidly presented (stimulus onset asynchronies = 250–750 msec) in the lower visual field. Each bilateral stimulus consisted of a small (alternating) checkerboard array in each lower visual field, with each array having either one, two, or no small dots (Fig. 1). In the active attention conditions, subjects attended covertly to either one side or the other of the bilateral stimuli and pressed a button in the right hand upon detecting ''target'' stimuli, which were those having checkerboard arrays on that side with two dots. (Those with only one or no dots in the array on that side were thus nontargets, or ''standards.'')

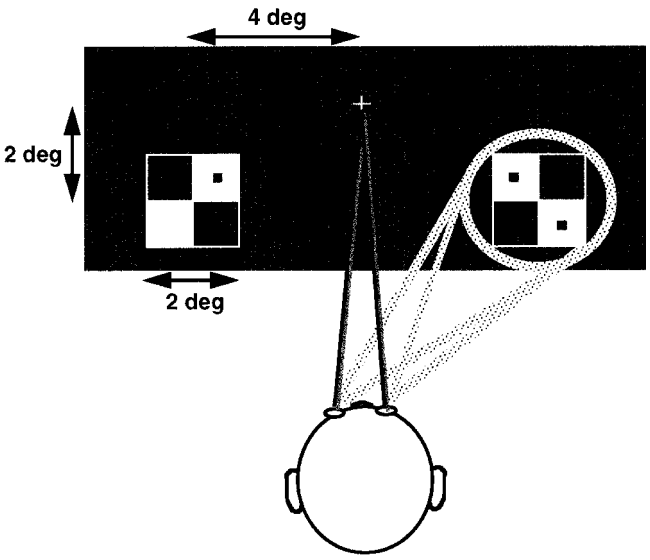

Figure 1.
Schematic diagram of the bilateral lower-visual-field stimulus and the visual spatial attention task, shown for an attend-right condition.

There were five conditions:

(1) attend left, with many targets (16%);
(2) attend right, with many targets (16%);
(3) attend left, with few targets (2%);
(4) attend right, with few targets (2%);
(5) passive viewing (with 2% irrelevant targets).

The present report focuses only on the occipital effects of the lateralized attention manipulations.

In preliminary runs, the target difficulty was adjusted for each subject, for each visual field, so that highly focused attention was required but such that target detection accuracy was around 90%. This was done by changing either the contrast and/or the size of the dots. These parameters were then used for both the ERP and PET runs.

ERP recordings

ERPs were recorded in 40 runs (8 in each condition) from 64 electrode sites. Prior to the recording session, the positions of all the electrodes and of several fiducial skull landmarks were determined using a sonic-based three-dimensional (3D) digitizer. Sixty-four channels of EEG were continuously recorded (sample rate per channel = 400 Hz, bandpass = .01–100 Hz), including several for monitoring and recording eye movements for later artifact rejection. Averaged ERPs to the standards and targets under the various attention conditions were extracted by selective averaging. Repeated-measures analyses of variance (ANOVAs) of the mean amplitude of ERP components across specified latency ranges were performed. Spherical-spline interpolation was used to generate scalp topographies of ERP activities [Perrin et al., 1989].

PET

Brain blood flow was measured with ^{15}O-labeled water (half-life = 123 sec), administered as an intravenous bolus of 8–10 ml of saline containing 50–70 mCi. Each subject underwent a series of 10 independent PET blood-flow scans during a 3-hr scanning session, with 2 runs in each of the 5 conditions, presented in a counterbalanced order. Following global normalization, the individual scan images were motion-corrected (using the automated imaging registration (AIR) algorithms of Woods et al. [1992]), 3D-interpolated, and spatially normalized into proportional bicommissural coordinate space based on the Talairach Atlas [Fox et al., 1988; Talairach and Tournoux, 1988; Lancaster et al., 1995]. Like-condition scans were then averaged across subjects, and the resultant grand-averaged scans from relevant pairs of conditions were subtracted. Change distribution analysis [Fox et al., 1988] was used to assess the statistical significance of outliers identified in the averaged subtraction images. Cluster analysis incorporating an evaluation of both spatial extent and amplitude of brain responses was performed to enhance both sensitivity and specificity in identifying regional changes [Xiong et al., 1995]. Z-score PET rCBF-change images were derived and thresholded ($|z| > 2.5$), where the z-scores were with respect to standard deviation values that were calculated from noise images derived from like-state subtractions. These were then overlaid on the spatially normalized, grand-averaged MRI images from the same subjects.

MRI scans

All subjects had high-resolution (1 mm × 1 mm × 1.6 mm) MRI scans obtained from a 1.9T Elscint MRI scanner. These were acquired using 3D-acquisition, T1-weighted, gradient-echo pulse sequences, with parameters TR = 33 msec, TE = 7.9 msec, and flip angle = 25 deg. The MR scans were also spatially normalized into Talairach coordinate space for coregistration with the PET scans and to enable grand-averaging.

ERP source analysis

Source analysis was performed on the attentional difference waves, constrained by seeding with PET activation foci, using the BESA (brain electrical source analysis) program [Scherg, 1992]. This program places simulated dipoles in a three-shell spherical head model, and iteratively adjusts their locations and orientations to try to achieve the best fit between the observed scalp potential distributions and the distributions that the model dipoles would produce. This approach is facilitated by the use of additional information, which in this study consisted of PET activation foci that were used were to seed (i.e., begin) the source analysis iterations. For each subject, coregistration of the ERP electrode reference frame with the MRI reference frame was accomplished by transformation matrices derived from common fiducial points in the two reference frames. For source analysis of the grand-average ERP waveforms, the combination of the ERP-to-MRI coregistration transforms and the MRI-to-Talairach spatial-normalization transforms (see MRI Scans, above), above allowed the electrode positions for each subject to be spatially normalized into Talairach space and then grand-averaged. The Talairach-space grand-average electrode locations, along with the Talairach-space PET activation foci for seeding, were then transformed into BESA space for the source analysis.

RESULTS

ERP effects

The ERPs showed significantly enhanced scalp-positive waves from 80–150 msec over occipital areas for all stimuli (i.e., both standards and targets) in all the attention conditions relative to passive. This early ''P1'' attention effect was larger contralateral to the direction of attention, such that there was a highly

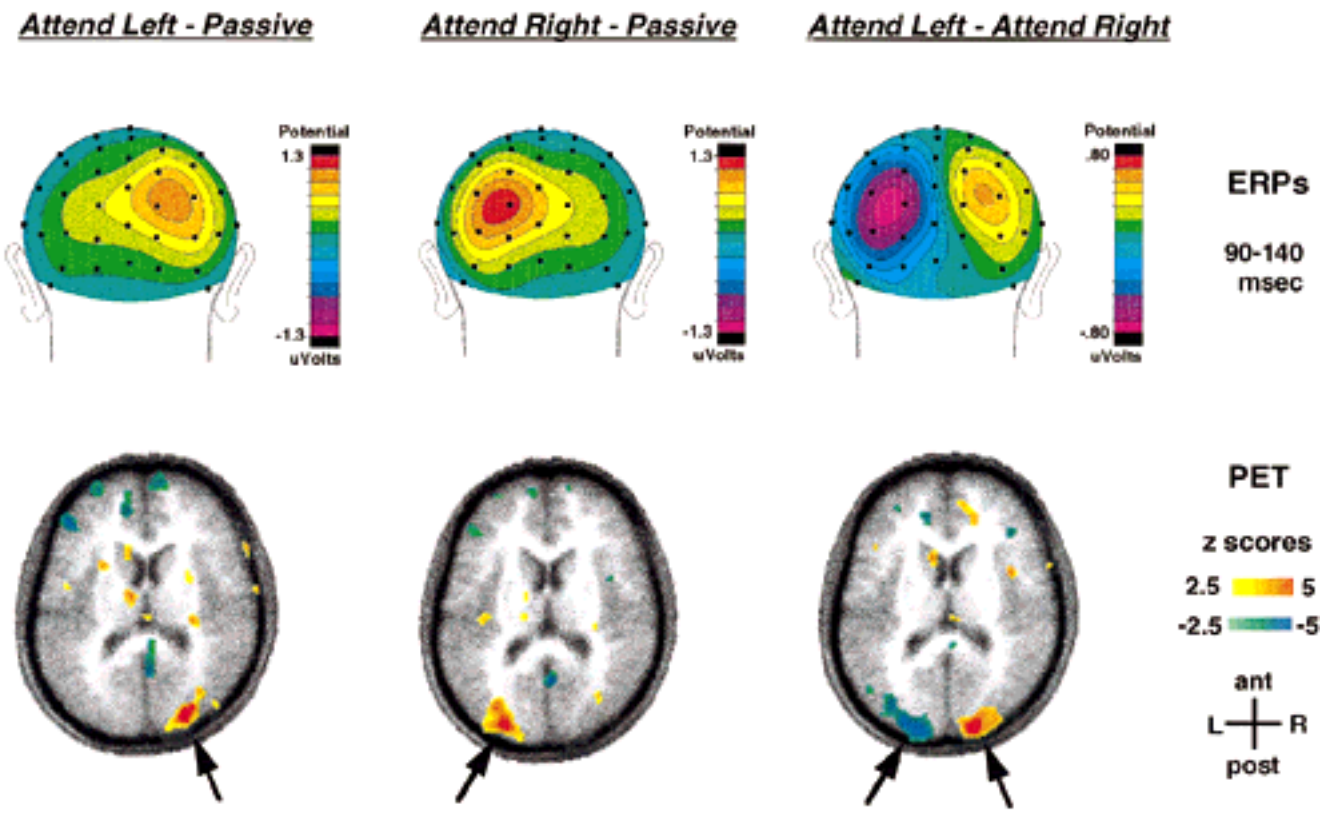

Figure 2.

Effects of lateralized attention to bilateral stimuli in the lower visual field. **Top:** Topographic distributions of the grand-average ERP difference waves derived from the attend-left, attend-right, and passive conditions, showing the effects of lateralized attention during the P1 latency range (90–140 msec). Because the P1 effects did not differ as a function of target frequency, ERPs were collapsed across this factor. **Bottom:** Grand-average z-score PET difference images showing the corresponding blood-flow changes due to lateralized attention, overlaid on the grand-averaged, spatially normalized MRI images from the same subjects. Images are horizontal scans through the dorsal occipital cortex (Talairach coordinate z = 12 mm). As with the ERPs, data were collapsed over the target frequency factor.

significant two-way interaction of attention direction × hemisphere ($P < 0.001$). These attention effects were not different between the many-target and few-target conditions, thus providing evidence that sustained attention was similar across these conditions.

Focusing on the effects of attention in the P1-latency range, attentional difference waves were derived and the topographic distribution of these around the peak of the P1 were calculated (Fig. 2, top). Keeping in mind that the eliciting stimuli in each of the conditions were identical and bilateral, Figure 2 clearly shows that, relative to passive viewing, attending to the left side of the stimuli results in a positive-wave peak over the right (i.e., contralateral) occipital cortex, and that attending to the right gave a positive peak over the left occipital cortex. An additional subtraction of attend-left minus attend-right ERPs was also performed, as this subtraction subtracts out nonspecific effects such as arousal. This subtraction yielded a distribution with two focal peaks of opposite polarities over the two occipital cortices (Fig. 2, top right).

PET effects

In the PET images, all active attention conditions relative to passive showed strong activations in the contralateral dorsal occipital areas (Brodmann areas 18/19: cuneus gyrus/middle occipital gyrus) (Fig. 2, bottom; Table I), which were similar in the many-target and few-target conditions and are thus associable with sustained attention and the focal early ERP positivity effect. Some weaker attention-related activation was

TABLE I. Talairach coordinates of centroids of occipital PET activations in attend-left-minus-attend-right subtraction

Activation	Structure	Increase / decrease	x	y	z
Dorsal occipital	Left cuneus / middle occipital	Decrease	−28	−89	+6
Dorsal occipital	Right cuneus / middle occipital	Increase	+18	−91	+12
Ventral occipital	Left fusiform	Decrease	−45	−71	−9
Ventral occipital	Right fusiform	Increase	+26	−75	−11

also observed in the contralateral ventral occipital cortex (fusiform gyrus) (Table I).

The extent of the PET effects in the dorsal occipital cortex suggested that these effects covered more than just one functional area. The effects did not appear to include any parts of the calcarine sulcus, indicating that there was no significant effect on V1 (primary visual cortex). In the attend-left-minus-attend-right subtraction, however, the effects did extend inferiorly and medially to within a centimeter of the calcarine, and thus may have included V2. From this most inferior and medial edge of the activation, the activated area extended superiorly, anteriorly, and laterally in a roughly C-shaped curve. The extent of the activation was greater on the left, especially in the lateral dimension.

PET-seeded ERP source modeling

The contralateral occipital PET attention effects, especially the strong dorsal occipital ones, and the contralateral ERP activations, especially the strong early positivity (P1 effect), were clearly experimentally associated (Fig. 2). However, to draw tighter connections between these hemodynamic and electrical changes requires a more formal modeling approach. To address the question of whether the PET activation areas are viable candidates as sources for the electrical effects, PET-seeded, iterative, dipole source modeling (BESA) was applied to the attend-left-minus-attend-right difference waves, focusing on the latency range of the P1 attention effect. This set of difference waves was viewed as the best to use for modeling, because not only does this subtraction control for nonspecific effects, such as arousal, but it also substantially reduced the complexity of the ERP effects. (Indeed, the attend-left-minus-attend-right ERP subtraction resulted in quite focused activity that was almost exclusively over the back of the head.) In addition, this subtraction greatly reduced the number of likely candidate dipole sources, in that there were considerably fewer PET activation hot spots in the corresponding attend-left-minus-attend-right PET subtraction relative to any of the PET subtractions of active attention minus passive.

Dipoles were first placed at the centroids of the largest PET activations in this subtraction, namely the dorsal occipital foci (Table I), and the orientations (but not locations) were allowed to vary. This orientation-only modeling yielded an extremely good fit for the P1 attention effect, explaining all but 3% of the distribution at the peak of the effect (110–130 msec). When location was also allowed to vary, the dipoles moved slightly anterior (5–8 mm) and explained all but 2% of the P1 effect (Fig. 3). In contrast, dipoles placed in the ventral occipital PET foci (Table I), with only orientation allowed to vary, gave a poor fit, leaving more than 16% of the P1 effect unexplained. When location was also allowed to vary, the dipoles moved upward during the iterative dipole fitting, stabilizing in the dorsal occipital locations. This modeling behavior strongly suggests that the dorsal occipital PET locations include the major contributing sources of the ERP P1 attention effect.

DISCUSSION AND CONCLUSIONS

Lateralized attention to lower-field bilateral visual stimuli resulted in increased activity in the contralateral dorsal occipital cortex. This relatively large activation appears to reflect attention-related enhancement in several of the early lower-field visual areas past V1 (e.g., V2, V3, V3a, dorsal V4) and appears to contain a major source(s) of the P1 ERP attention effect that peaks at 120 msec. These dorsal occipital effects do not appear to include V1 (primary visual cortex) itself, but the proximity to the calcarine fissure suggests that they may include V2. The additional smaller effect in the fusiform gyrus seen in the present experiment may reflect some activation of the ventral pathway for object analysis or other higher-order processing, al-

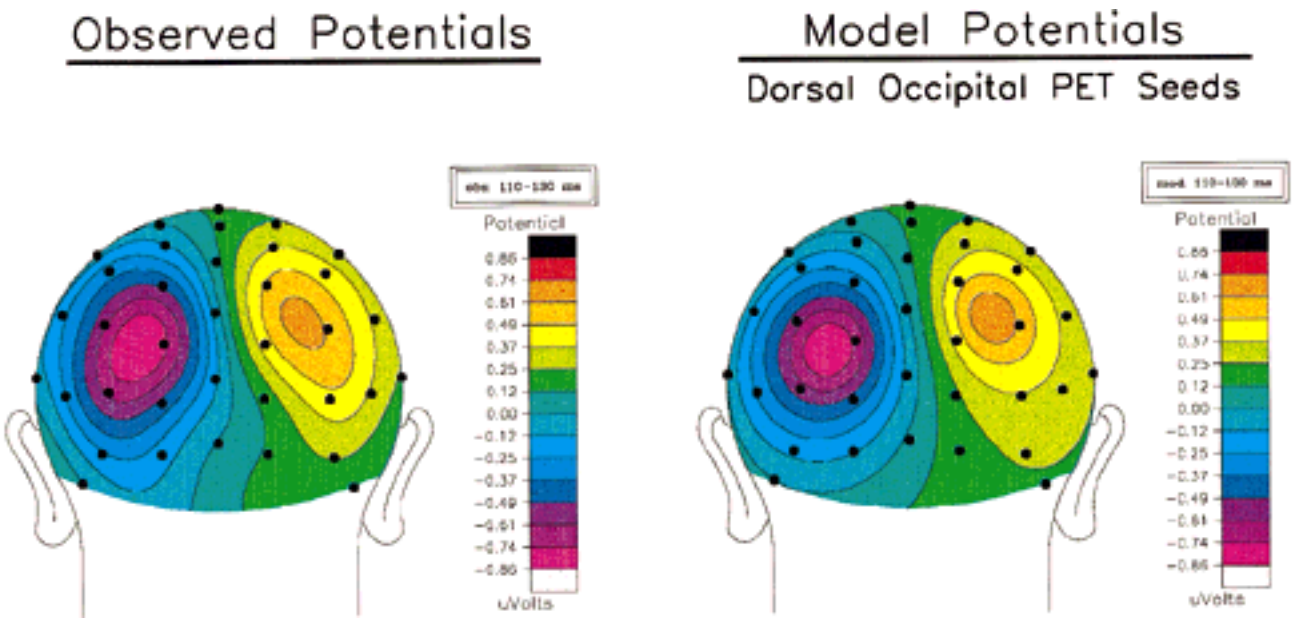

Figure 3.
Left: Observed potential distributions in the attend-left-minus-attend-right difference waves at the peak of the P1 attention effect (110–130 msec). **Right:** Corresponding model potential distributions seeded by the dorsal occipital PET foci, which provided an excellent fit to the P1 effect (residual variance 2%).

though the timing and contribution to the ERP attention effects (for lower-field stimuli) are not yet clear.

In contrast, in the Heinze et al. [1994] study, focused visual spatial attention toward one side of upper-field bilateral stimuli resulted in effects that were only in the ventral contralateral occipital cortex (fusiform), with no effects in the dorsal occipital cortex. Although the task in Heinze et al. [1994], like the present one, involved very focused visual spatial attention, it also included substantial object analysis, which could have biased the effects in the former study toward ventral occipital activation. However, these strong ventral effects (and the lack of dorsal ones) have now been replicated [Mangun et al., this issue] in a task involving much less object analysis. We suggest that these fusiform gyrus PET effects in these upper-visual-field attention studies actually consist of a combination of retinotopically organized effects in early (e.g., VP, V4) upper-field visual areas (which produce the upper-field ERP P1 effect) *plus* effects in adjacent higher-order areas in the ventral processing stream, blurring together as a large PET activation in the contralateral ventral occipital cortex. In contrast, the use of lower-field stimuli in the present experiment appears to have resulted in a separation between effects in the early visual areas that have a split representation (and are dorsal for lower-field stimuli) and the higher-order ventral-stream effects (which are ventral for both upper- and lower-field stimuli).

Dipoles seeded into the dorsal occipital PET foci in the present study yielded an excellent fit for the ERP P1 attention effect. In contrast, dipoles constrained to the fusiform foci did not provide a good fit for the P1 effect, and, when the location constraints were released, the dipoles moved upward to the dorsal occipital locations. These modeling results argue that the dorsal occipital PET foci are major contributors to the early ERP P1 attention effect for lower-visual-field stimuli. Thus, these early-latency attention-related enhancements also follow the retinotopic organization of the visual sensory input pathways. The location of these effects (beginning as early as V2), in conjunction with their very-early-onset latency (70–80 msec) and their retinotopic organization, suggests that these effects may be a reflection of enhanced activity on the initial ascending input activation. Thus, these combined PET/ERP data provide strong evidence that sustained visual spatial attention results in a preset, top-down, positive biasing of the early sensory input channels in a retinotopically organized way.

ACKNOWLEDGMENTS

We thank B. Heyl, J. Ruby, and Dr. J. Xiong for valuable technical assistance, and Dr. G.R. Mangun, Dr. M. Liotti, and the reviewers for a number of helpful comments. This work was supported by a grant from the Research Imaging Center.

REFERENCES

Fox PT, Mintun MA, Reiman EM, Raichle ME (1988): Enhanced detection of focal brain responses using inter-subject averaging and change-distribution analysis of subtracted PET images. J Cereb Blood Flow Metab 8:642–653.

Heinze HJ, Mangun GR, Burchert W, Hinrichs H, Scholz M, Muente TF, Gos A, Scherg M, Johannes S, Hundeshagen H, Gazzaniga MS, Hillyard SA (1994): Combined spatial and temporal imaging of brain activity during visual selective attention in humans. Nature 372:543–546.

Hillyard SA, Mangun GR, Woldorff MG, Luck SJ (1995): Neural systems mediating selective attention. In MS Gazzaniga (Ed.), The Cognitive Neurosciences, Cambridge, MA: MIT Press, pp. 665–681.

Hillyard SA, Picton TW (1987): Electrophysiology of cognition. In: Mountcastle VB (ed): Handbook of Physiology: Section 1: The Nervous System, Volume 5: Higher Brain Functions. Baltimore: American Physiological Society, pp 519–584.

Lancaster JL, Glass TG, Lankipalli BR, Downs H, Mayberg H, Fox PT (1995): A modality-independent approach to spatial normalization of tomographic images of the human brain. Hum Brain Mapping 3:209–223.

Mangun GR, Hopfinger J, Kussmaul CL, Fletchert E, Heinze HJ (1997): Covariations in ERP and PET measures of spatial selective attention in human extrastriate visual cortex. Human Brain Mapping, 5:273–279.

Perrin FJ, Pernier O, Bertrand O, Echallier JF (1989): Spherical splines for scalp potential and current density mapping. Electroencephalogr Clin Neurophysiol 72:184–187.

Posner MI, Raichle M (1994): Images of Mind, New York: Scientific American Library, pp. 152–179.

Scherg M (1992): Functional imaging and localization of electromagnetic brain activity. Brain Topo 5:103–111.

Sereno MI, Dale AM, Reppas JB, Kwong KK, Belliveau JW, Brady TJ, Rosen BR, Tootell RBH (1995): Borders of multiple visual areas in humans revealed by functional magnetic resonance imaging. Science 258:889–893.

Talairach J, Tournoux P (1988): Co-Planar Stereotaxic Atlas of the Human Brain. New York: Thieme.

Ungerleider L, Haxby JV (1994): ''What'' and ''where'' in the human brain. Curr Opin Neurobiol 4:157–165.

Woods RP, Cherry SR, Mazziotta JC (1992): Rapid automated algorithm for aligning and reslicing PET images. J Comput Assist Tomogr 16:622–633.

Xiong J, Gao JH, Lancaster JL, Fox PT (1995): Clustered pixels analysis for functional MRI activation studies of the human brain. Hum Brain Mapping 3:287–301.

Zeki S (1993): A Vision of the Brain. London: Blackwell.